Interlayer transition zones in Mo/Si superlattices

S. Yulin,[a] T. Feigl, T. Kuhlmann, and N. Kaiser
Fraunhofer-Institut für Angewandte Optik und Feinmechanik, Schillerstrasse 1, D-07745 Jena, Germany

A. I. Fedorenko, V. V. Kondratenko, O. V. Poltseva, V. A. Sevryukova,
A. Yu. Zolotaryov, and E. N. Zubarev
National Technical University "Kharkiv Polytechnic Institute", Kharkiv, 310002, Ukraine

The formation of interlayer transition zones (ITZs) in sputtered Mo/Si multilayer structures was studied by means of cross-section electron microscopy and grazing incidence reflectivity measurements. For the evaluation and calculation of interface effects the multiperiodic design of Mo/Si structure was used. It was found that the thickness asymmetry of ITZs (Mo-on-Si and Si-on-Mo) in Mo/Si multilayer structures depends on the degree of perfection of the crystalline structure of the molybdenum layer. A transition from asymmetrical to symmetrical ITZs with a disordering of the molybdenum crystalline structure was shown. A model for the formation mechanism of asymmetrical ITZs at the different interfaces in Mo/Si multilayer structures is suggested. According to this model, ITZ formation at the Mo-on-Si interface is controlled by the surface diffusion of Si atoms on the growing molybdenum surface. In contrast, ITZ formation at the Si-on-Mo interface is determined by the bulk diffusion of Si atoms in textured molybdenum grains. © *2002 American Institute of Physics.* [DOI: 10.1063/1.1487919]

I. INTRODUCTION

The wide application of transition metal silicides in the semiconductor industry has stimulated comprehensive studies of interaction processes at interfaces in systems like "transition metal-silicon" (t-Me/Si).[1,2] As a rule, all t-Me/Si systems have a few silicide phases in binary phase diagrams. This fact indicates a high chemical reactivity and miscibility of the corresponding elements at the interfaces, which automatically causes an interface broadening with the formation of interlayer transition zones (ITZs). The formation of such ITZs at the first stage of a metal film deposition on single-crystalline, poly-crystalline or amorphous silicon has been observed for different deposition technologies. Thus, two main questions have to be addressed: (i) What is the formation mechanism and the chemical composition of ITZs? and (ii) Is it possible to predict the thickness of ITZs before deposition, and what are the factors effecting the ITZ formation?

In recent years, a remarkable success in x-ray multilayer optics has stimulated additional interest in a detailed understanding of the above mentioned questions. In particular, multilayer mirrors (MMs) are widely used as effective reflective elements for the extreme-ultraviolet (EUV) and soft x-ray wavelengths ($1 \text{ nm} < \lambda < 40 \text{ nm}$). Due to its high experimental reflectivity ($R > 69\%$) at 13.4 nm,[3] Mo/Si is a promising material combination for MMs to be applied in EUV lithography. The reflective properties of Mo/Si mirrors depend substantially on the structure of ITZs, especially on their thickness and composition. Using high-resolution transmission electron microscopy (HRTEM), Petford-Long *et al.*[4]

discovered the presence of amorphous ITZs between pure layers of Mo and Si in superlattices prepared by magnetron sputtering. It has been shown by several authors[4–8] that the Mo-on-Si interface is thicker than the Si-on-Mo one. Some results of these studies are summarized in Table I. It has to be mentioned that the formation of asymmetrical ITZs is independent of the deposition technology (electron beam evaporation or magnetron sputtering). The fact that asymmetrical ITZs have been observed in specimens deposited under extremely different conditions implies that it may be an intrinsic property of the Mo–Si couple. Furthermore, it has been shown that the asymmetry itself can vary significantly with the substrate temperature[8] and substrate bias.[9] Moreover, symmetrical as well as slightly asymmetrical interlayers have been observed in different Si-based multilayer systems such as Ti/Si,[10] Ru/Si,[7] and Sc/Si.[11]

Although the interlayers themselves can be well observed by HRTEM, this method is not sensitive to their phase compositions.[12] The composition of silicides at the interfaces can be identified by structure analysis methods (electron or x-ray diffraction) or by chemical composition analysis methods (Auger spectroscopy, secondary ion mass spectroscopy, x-ray fluorescence spectroscopy, etc.). But all these methods have considerable limitations if the interlayers are amorphous and very thin ($t_{ITZ} \sim 1 \text{ nm}$). Holloway and Sinclair have demonstrated the faculty of HRTEM as an indirect method for the determination of the phase composition of ITZs in Ti/Si superlattices.[10] The method is based on the analysis of HRTEM images before and after annealing. Due to the activation of interdiffusion processes under heat load and corresponding changes in the layer thickness, the phase composition of ITZs can be calculated. Additionally, it has been confirmed that it is possible to estimate the phase composition of ITZs for superlattices in the as-deposited state if

[a]Author to whom correspondence should be addressed; electronic mail: yulin@iof.fraunhofer.de

TABLE I. Growth conditions and thickness ($t_{\text{Mo-on-Si}}$ and $t_{\text{Si-on-Mo}}$) of interlayer transition zones in Mo/Si multilayers.

References	Deposition method	Period, d (nm)	Substrate temperature (°C)	$t_{\text{Mo-on-Si}}$ (nm)	$t_{\text{Si-on-Mo}}$ (nm)
A. K. Petford-Long et al.[a]	dc-magnetron	7.0–1.2	20	1.7(±0.3)	1.0(±0.3)
K. Holloway et al.[b]	Mo-dc, Si-rf	13.0	20	1.9	1.1
D. G. Stearns et al.[c]	rf-magnetron	11.0	20	1.0	0.7
D. L. Windt et al.[d]	dc-magnetron	6.8–7.5	20	1.2	1.0
M. B. Stearns et al.[e]	*e*-beam	12.9	20	1.5(±0.3)	0.6(±0.3)
	evaporation	9.2	200	1.8(±0.3)	0.7(±0.2)
		8.6	300	2.3(±0.2)	0.5(±0.3)

[a]See Ref. 4.
[b]See Ref. 5.
[c]See Ref. 6.
[d]See Ref. 7.
[e]See Ref. 8.

(i) the deposition rates are precisely known, and (ii) the thicknesses of all layers are measured by means of HRTEM images. As a result, an atomic ratio of 1:2 for Ti and Si for the ITZ composition in the as-deposited Ti/Si superlattice has been determined.[10] Similar HRTEM studies have been performed for Sc/Si superlattices.[11] It has been found that slightly asymmetrical ITZs of ScSi composition are formed at the interfaces in the Sc/Si superlattice.

The Mo/Si multilayer structure differs from other t-Me/Si systems in the strong thickness asymmetry of ITZs (Table I), and in the big difference in the behavior of Mo-on-Si and Si-on-Mo interlayers under heat load.[5] In previous work[13] it was suggested that a transition from the asymmetrical to the symmetrical type of ITZs in Mo/Si superlattices takes place in the case of a disordering of the crystalline structure of the Mo layer. The goal of current research is to present additional arguments for understanding the importance of structural effects on ITZ formation.

II. PREPARATION AND CHARACTERIZATION OF SAMPLES

The Mo–Si periodic structures were deposited by dc-magnetron sputtering on single-crystalline Si(111) wafers. The alternate layers of Mo and Si were deposited by successive exposure of the substrate under Mo and Si targets with an Ar pressure of 2×10^{-3} Torr. The thicknesses of the deposited Mo and Si layers were controlled by varying the power applied to the magnetron sources and the time of the substrate exposure under the corresponding target.

The Mo and Si deposition rates were estimated by the deposition of a double periodic multilayer system on the same substrate.[14] Low angle x-ray diffraction of Cu $K\alpha$ radiation of the double periodic multilayer system shows two sets of Bragg peaks, one for each multilayer periodic stack. The material rate can be calibrated accurately if two multilayer stacks differ from each other only by the deposition time of one material. For the determination of both Mo and Si rates two double periodic multilayer systems were deposited and investigated. After that a special multiperiodic structure was designed and deposited so that the bilayer period (d) increases from stack to stack and the thickness ratio Γ ($\Gamma = t_{\text{Mo}}/d$) remains constant for all stacks. A similar design was first used for studies of the material interaction in Mo_2C/Si superlattices by Barbee and Wall.[15] The design parameters of the multiperiodic structure are shown in Table II.

Ultrathin specimens for the HRTEM study were prepared by a two-step process of mechanical polishing and ion-beam milling as proposed by Bravman and Sinclair.[12] Ar^+ ions with energies of about 6 keV at the first stage and Xe^+ ions with energies of 2 keV at the final stage were used for the ion-beam milling of the specimens. All HRTEM studies were performed using a PEM-U electron microscope with a minimum line resolution of 0.2 nm. HRTEM images of all stacks were obtained with the same magnification (x 420 000), which was calibrated by a superlattice with known period. All images were obtained with a defocus of the objective lens of ~20 nm. This defocus value supports a significant improvement of the ITZ contrast and does not produce artifacts like Fresnel contours. Parallelism of the electron beam and interfaces was provided with a goniometer and controlled by the minimum measured Γ value and

TABLE II. Design of the multiperiodic structure. Period multilayer d_D, Mo layer thickness t_{Mo}^D, number of periods N and thickness ratio Γ_D, which were designed.

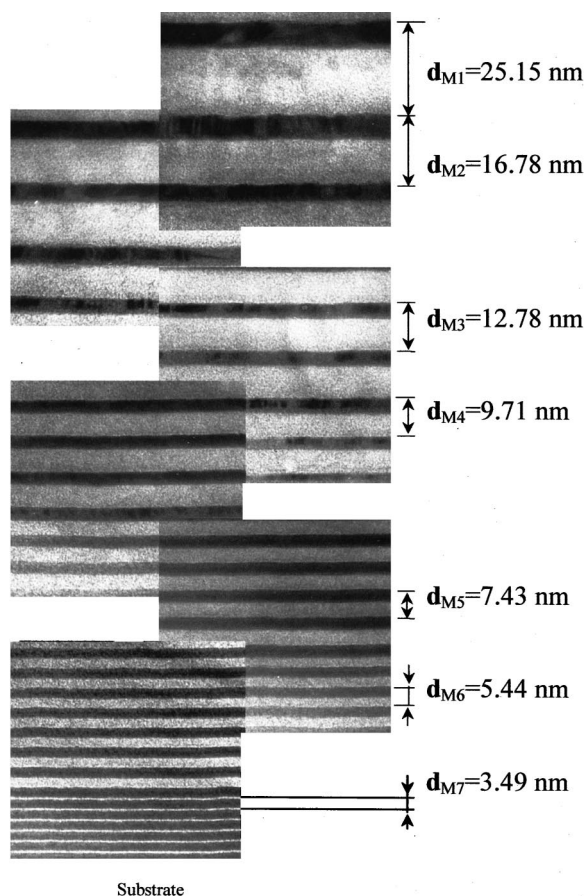| Parameter	Stack						
	1	2	3	4	5	6	7
d_D (nm)	26.4	17.8	13.4	10.25	8.03	5.88	3.74
t_{Mo}^D (nm)	5.9	4.0	3.0	2.3	1.81	1.33	0.85
Γ_D	0.223	0.225	0.224	0.224	0.225	0.226	0.227
N	10	10	15	20	25	30	50

FIG. 1. HRTEM images of different stacks in the Mo/Si multiperiodic structure. Measured period values for different multilayer stacks are shown.

FIG. 2. Dependence $\Gamma = f(d)$ in case of the real structure (with intermixing) ($\bigcirc$) and a structure without intermixing effect ($\bullet$).

the symmetry of Fresnel contours on opposite interfaces for each stack.

III. RESULTS

HRTEM images of all stacks are shown in Fig. 1. One can see that the measured ratio of the absorber layer thickness (containing Mo atoms) to multilayer period $\Gamma_M = (t_{Mo} + t_{ITZs})/d_M$ (where d_M is the period which was measured directly from HRTEM images) changes significantly with a decreasing superlattice period. The dependence $\Gamma_M = f(d)$ (Fig. 2) demonstrates the considerable intermixing between pure components at the interfaces. Without intermixing, this dependence would be a straight line with $\Gamma_D \approx 0.23$ as designed according to Table II (Γ_D is the designed ratio). At the same time, a contraction in d_M (Fig. 1) in comparison to the designed values d_D (Table II) was found. The observed contraction of d_M associated with the intermixing of Mo and Si suggests that ITZs are composed of a denser phase than the equivalent combination of Mo and Si bulk phases.

The HRTEM images of the various stacks differ in contrast. For stacks with $d_M \geq 9.7$ nm (stacks 1–4 in Fig. 1), the periodic structure consists of amorphous silicon (bright) and crystalline molybdenum (dark) layers. Mo grains are well highlighted by means of diffraction contrast and have a strong nonaxial shape. The grain dimension in the direction
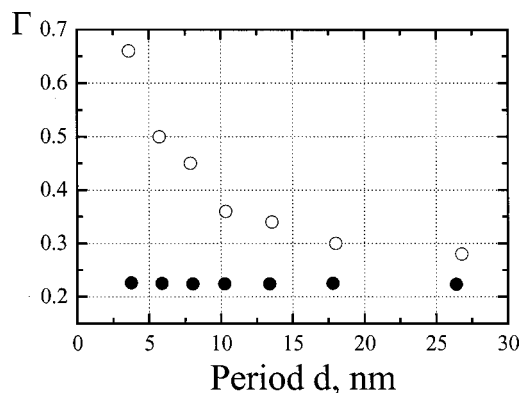
of the periodic structure is restricted by the Mo layer width, while in the lateral direction the length of some grains reaches ~40 nm. Mo grains are textured, and they are restricted by close-packed (110) plains oriented parallel to the interface. An axial texture is seen on the selected area diffraction pattern in the form of pronounced arcs on the diffraction circle, which corresponds to the most vivid bcc reflections from {110} planes. On the HRTEM images, the asymmetrical amorphous interlayers which are brighter than pure molybdenum and darker than pure silicon can be clearly seen between Mo grains and amorphous Si. Measurements of ITZ thicknesses were performed for stacks 1–4 (Table III).

With decreasing multilayer period ($d_M \leq 7.43$ nm: stacks 5–7 in Fig. 1), a remarkable difference in the layer structure has been observed. First, there is an obvious disproportion between the measured and designed ($\Gamma_D \approx 0.23$) thickness ratios of the components (Fig. 2). Second, the Mo grains show no diffraction contrast, which means that Mo layers have a noncrystalline structure. And finally, the images for stacks 5 and 6 show a weak-contrast dark stripe in the middle of the molybdenum layer (Fig. 1). This contrast can be explained by remaining molybdenum which is not participating in the silicide formation reaction. Additionally, it should be mentioned that no similar contrast (dark stripe) was observed in the $MoSi_2$/Si superlattices.[16] According to the Mo–Si binary phase diagram,[17] the $MoSi_2$ and Si components cannot react with each other by the formation of solid solutions and transition phases. If our assumption is correct, the ITZs in stacks 5 and 6 should be nearly symmetrical. A similar, though rather faint contrast can be distinguished in the molybdenum containing layers of stack 7 with a designed thickness $t_{Mo} = 0.85$ nm (see Table II). Apparently, a considerable

TABLE III. The measured thickness (from HRTEM images) of interlayer transition zones for Mo-on-Si and Si-on-Mo interfaces in stacks 1–4.

Thickness (nm)	Stack			
	1	2	3	4
$t_{Mo\text{-}on\text{-}Si}^M$	1.2 ± 0.25	1.2 ± 0.23	1.1 ± 0.26	1.3 ± 0.26
$t_{Si\text{-}on\text{-}Mo}^M$	0.7 ± 0.25	0.7 ± 0.23	0.6 ± 0.26	0.5 ± 0.26

TABLE IV. Comparison between designed (d_D, t_{Mo}^D, and Γ_D) and calculated (d_C, t_{Mo}^C, and Γ_C) multilayer parameters for two kinds of interlayers (of $MoSi_2$ composition): 1. The thicknesses of Mo-on-Si and Si-on-Mo interfaces are 1.2 and 0.6 nm, respectively. 2. The thicknesses of Mo-on-Si and Si-on-Mo interfaces are 1.2 and 1.2 nm, respectively.

Parameter	Stack						
	1	2	3	4	5	6	7
d_D (nm)	26.4	17.8	13.4	10.25	8.03	5.88	3.74
t_{Mo}^D (nm)	5.9	4.0	3.0	2.3	1.81	1.33	0.85
Γ_D	0.223	0.225	0.224	0.224	0.225	0.226	0.227
d_M (nm)	25.15	16.78	12.78	9.71	7.43	5.44	3.49
1. d_C (nm)	25.82	17.45	13.45	10.38	8.1	6.11	4.16
t_{Mo}^C (nm)	5.53	3.72	3.02	2.39	2.39	2.03	1.36
Γ_C	0.21	0.21	0.225	0.23	0.3	0.33	0.33
2. d_C (nm)					8.33	6.34	4.39
t_{Mo}^C (nm)					2.02	1.66	0.99
Γ_C					0.24	0.26	0.23

fraction of molybdenum in this stack has reacted with Si by the formation of amorphous silicide.

IV. DISCUSSION

The results of processing the data extracted from the HRTEM images (Fig. 1) are summarized in Table IV. The key goal of our calculations was to obtain from measured HRTEM data (d_M, t_{Mo}^M,...) the calculated values for d_C, t_{Mo}^C and $\Gamma_C = t_{Mo}^C / d_C$, assuming that there is not a chemical interaction between Mo and Si. In Table IV these values are compared with the designed ones. Considering the results of the direct measurement of ITZs for stacks 1–4 (see Table III), we assumed in our calculations that the ITZ thickness is 1.2 nm for the Mo-on-Si and 0.6 nm for the Si-on-Mo interface. Due to the low ITZ contrast of stacks 5 and 6, it is not possible to measure their thickness precisely, but the presence of the darker stripe in the middle of the molybdenum-containing layer allows us to assume a similar thickness for ITZs of both interface types. Thus, for stacks 5–7, the ITZs for both interface types were assumed to be of equal thickness ($t_{Mo-on-Si} = t_{Si-on-Mo} = 1.2$ nm). It was also supposed that all ITZs have a phase composition close to $MoSi_2$ (additionally, Mo_5Si_3 and Mo_3Si have been tested). This does not contradict the Walser-Bené rule.[18] In addition it was found[5,6] that during annealing of Mo/Si/Mo...superlattices, the ITZs crystallize into Mo_2Si silicide. It has also been demonstrated by Auger spectroscopy that amorphous silicide of the composition $MoSi_2$ forms at the surface at the beginning of Mo deposition (first 0.4 nm) on the Si substrate at a temperature of $60\,°C < T_{sub} < 200\,°C$.[19]

If the densities of the pure components and silicides are known, it is possible to calculate the values of d_C, t_{Mo}^C and Γ_C. For our calculations we used the following densities: $\rho_{Si} = 2.3$ g/cm^3, $\rho_{Mo} = 10.2$ g/cm^3, and $\rho_{MoSi_2} = 6.24$ g/cm^3 ($\rho_{Mo_5Si_3} = 8.24$ g/cm^3 and $\rho_{Mo_3Si} = 8.97$ g/cm^3). In Table IV, for stacks 5–7, the parameters d_C, t_{Mo}^C, and Γ_C are shown for the asymmetrical ($t_{Mo-on-Si} = 1.2$ nm, $t_{Si-on-Mo} = 0.6$ nm) and symmetrical ($t_{Mo-on-Si} = t_{Si-on-Mo} = 1.2$ nm) types of ITZ with a fixed $MoSi_2$ composition. The dependence Γ_C

$= f(d_C)$ for the symmetrical and asymmetrical ITZ types is shown in Fig. 3. As it is seen from Table IV, and Fig. 3, the calculated values the t_{Mo}^C and Γ_C values are much closer to the designed values if the formation of symmetrical ITZs of $MoSi_2$ composition is assumed for stacks 5–7. For other silicides (for example Mo_3Si or Mo_5Si_3), the same calculations yield a less good agreement between the calculated and designed values.

On the basis of the data presented here, and with the published results taken into account, different formation mechanisms for the ITZs at the Mo-on-Si and Si-on-Mo interfaces can be suggested. Due to the high formation heat of the transition metals silicides, a strong interaction between molybdenum and silicon films and a layer-by-layer growth mode can be expected. Slaughter *et al.*[19] have shown by the use of low-energy electron diffraction that the diffraction from single-crystalline Si completely vanishes after a deposition of only ~0.2 nm Mo on the Si substrate. This fact indicates that the surface becomes amorphous under Mo deposition, i.e., that amorphous silicide grows in a layer-by-layer mode. The predominating diffusant in the Mo–Si binary system is silicon.[1,2] For a long time it was unclear
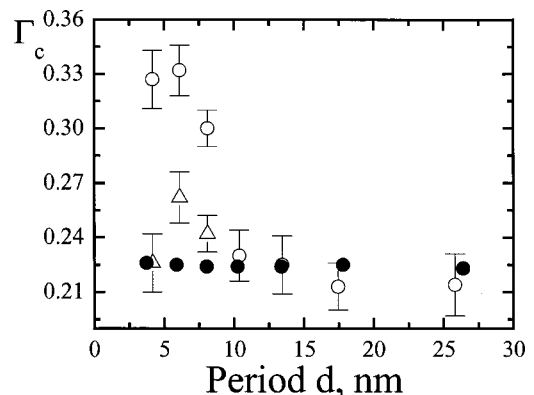

FIG. 3. Dependence $\Gamma_C = f\,(d_C)$, with the assumption that asymmetrical interlayers with 1.2 and 0.6 nm thicknesses (○) and symmetrical interlayers of 1.2 nm fixed thickness (△) are formed (all interlayers are of $MoSi_2$ composition). $\Gamma_D \approx 0.23$ (●) is shown for comparison.

how Si atoms can break the strong covalent bonds and diffuse into the growing metallic layer at such low temperatures ($T < 200\,°C$). Using tunneling microscopy, Bedrossian[20] has shown that the Mo atoms penetrate into certain crystallographic positions of single-crystal (100) Si and assist in breaking the Si covalent bonds. In this case, the Mo atoms cover the surface of amorphous silicon homogeneously, and the released Si atoms diffuse along the growing Mo film. As it has been shown, a low activation energy of the surface diffusion of Si (~ 0.2 eV)[8] stimulates in an intensive intermixing between Mo and Si. The presence of nanoscale roughness on the free surface of amorphous silicon[21] also assists in the breaking of Si covalent bonds and atomic intermixing. When the atomic ratio of the pure components in a local area reaches 1:2, clusters of amorphous disilicide are formed. A molybdenum layer of about 0.5 nm will be enough for the formation of ITZ with a thickness of 1.2 nm. When the thickness of the silicide layer reaches about 1.2 nm, it becomes a diffusion barrier for Si atoms. A further increase of the ITZ thickness at the Mo-on-Si interface is possible only due to silicon bulk diffusion through the silicide layer.

The ITZ at the Si-on-Mo interface is formed under completely different conditions if a Mo layer with a good texture is already formed. In our experiments, the transition from the amorphous to the polycrystalline textured structure of the Mo layers is observed for $t_{Mo}^{D} \geq 2.3$ nm. In this case, the Si atoms arriving at the molybdenum surface can penetrate into the textured Mo grains mainly due to bulk diffusion. The bulk diffusion coefficient is very low for the Si atoms in the low-temperature range. As a result, a thin and homogeneous ITZ with thickness $t_{Si-on-Mo} \approx 0.6$ nm is formed at the Si-on-Mo interface.

When $t_{Mo}^{D} < 2.3$ nm, the molybdenum layer structure becomes amorphous (or nanocrystalline) with a high density of defects. It is possible to predict higher diffusion coefficients for Si atoms inside the disordered (amorphous) Mo layer than inside high-textured molybdenum. Due to higher diffusion coefficients, thicker ITZs with a thickness of $t_{Si-on-Mo} \approx 1.2$ nm are formed. When the ITZ reaches a thickness of $t_{Si-on-Mo} \geq 1.2$ nm, this layer becomes a diffusion barrier for Si atoms.

It is clear that the final ITZ thickness in the Me/Si system is determined by the penetrability of the silicide layer to the diffusing components in certain deposition conditions. This penetrability depends on the substrate temperature and the energy of the atoms arriving at the surface. That is the reason why the ITZ thickness is different for the different Me/Si superlattices, and as a rule it is larger if the metal has a lower melting temperature.

V. CONCLUSION

A helpful HRTEM-based method for an estimation of the chemical composition of amorphous intermixed zones in as-deposited Mo–Si superlattices has been developed. A model for the formation mechanism of asymmetrical ITZs at the different interfaces in Mo/Si superlattices has been suggested. According to this model, the ITZ formation at the Mo-on-Si interface is controlled by the surface diffusion of Si atoms on the growing molybdenum surface. In contrast, the ITZ formation at the Si-on-Mo interface is determined by bulk diffusion of Si atoms in perfectly textured molybdenum grains. As a result, asymmetrical ITZs with thicknesses of $t_{Mo-on-Si} \approx 1.2$ nm and $t_{Si-on-Mo} \approx 0.6$ nm are formed, given a molybdenum thickness of $t_{Mo} \geq 2.3$ nm. The atomic ratio of components inside both ITZs is close to 1:2 for Mo and Si, respectively, and corresponds to disilicide molybdenum. Symmetrical ITZs with a thickness of $t_{Mo-on-Si} = t_{Si-on-Mo} = 1.2$ nm and a $MoSi_2$ phase composition are formed on both interfaces when the structure of the Mo layer becomes strongly disordered (0.9 nm $< t_{Mo} < 2.3$ nm).

[1] S. P. Murarka, *Silicides for VLSI Applications* (Academic, Orlando, 1983).
[2] K. N. Tu, and J. W. Mayer, in *Thin Films-Interdiffusion and Reactions*, edited by L. M. Poate, K. N. Tu, and J. W. Mayer (Wiley, New York, 1978).
[3] E. Louis *et al.*, Proc. SPIE **4146**, 60 (2000).
[4] A. K. Petford-Long, M. B. Stearns, C.-H. Chang, R. S. Nutt, D. G. Stearns, N. M. Seglio, and A. M. Hawryluk, J. Appl. Phys. **61**, 1422 (1987).
[5] K. Holloway, K. B. Do, and R. Sinclair, J. Appl. Phys. **65**, 474 (1989).
[6] D. G. Stearns, M. B. Stearns, Y. Cheng, J. H. Stith, and N. M. Ceglio, J. Appl. Phys. **67**, 2415 (1990).
[7] D. L. Windt, R. Hull, and W. K. Waskiewicz, J. Appl. Phys. **71**, 2675 (1992).
[8] M. B. Stearns, C.-H. Chang, and D. G. Stearns, J. Appl. Phys. **71**, 187 (1992).
[9] S. P. Vernon, D. G. Stearns, and R. S. Rosen, Appl. Opt. **32**, 6969 (1993).
[10] K. Holloway and R. Sinclair, J. Less-Common Met. **140**, 139 (1988).
[11] Yu. A. Uspenskii, V. E. Levashov, A. V. Vinogradov, A. I. Fedorenko, V. V. Kondratenko, Yu. P. Pershin, E. N. Zubarev and V. Yu. Fedotov, Opt. Lett. **23**, 771 (1998).
[12] J. C. Bravman and R. Sinclair, J. Electron Microsc. Tech. **1**, 53 (1984).
[13] E. N. Zubarev, V. V. Kondratenko, O. V. Poltseva, V. A. Sevrukova, A. I. Fedorenko, and S. A. Yulin, Metallofiz. Noveishie Tekhnol. **19**, 56 (1997) [in Russian].
[14] C. Montcalm, B. T. Sullivan, H. Pepin, J. A. Dobrowolski, and M. Sutton, Appl. Opt. **33**, 2057 (1994).
[15] T. W. Barbee, Jr. and M. Wall, Proc. SPIE **3113**, 204 (1997).
[16] A. I. Fedorenko, A. S. Garbuz, V. V. Kondratenko, Yu. P. Pershin, V. E. Pukha, O. V. Poltseva, S. A. Yulin, E. N. Zubarev, Proc. SPIE **2453**, 15 (1995).
[17] M. Hansen and K. Anderko, *Structure of Binary Alloys* (Metallurgizdat, Moscow, 1962).
[18] R. M. Walser and R. W. Bené, Appl. Phys. Lett. **28**, 624 (1976).
[19] J. M. Slaughter, A. Shapiro, P. A. Kearney, and C. M. Falko, Phys. Rev. B **44**, 3854 (1991).
[20] P. D. Bedrossian, Surf. Sci. **320**, 247 (1994).
[21] D. B. Boercker and W. L. Morgan, Proc. SPIE **1547**, 47 (1991).